Lightning and Severe Weather: A Comparison between Total and Cloud-to-Ground Lightning Trends

CHRISTOPHER J. SCHULTZ

Department of Atmospheric Science, University of Alabama in Huntsville, Huntsville, Alabama

WALTER A. PETERSEN

NASA Marshall Space Flight Center, Huntsville, Alabama

LAWRENCE D. CAREY

Earth System Science Center, University of Alabama in Huntsville, Huntsville, Alabama

(Manuscript received 22 September 2010, in final form 6 April 2011)

ABSTRACT

Many studies over the past several decades have attempted to correlate trends in lightning (e.g., rates, polarity) to severe weather occurrence. These studies mainly used cloud-to-ground (CG) lightning information due to the ease of data availability, high detection efficiency, and broad coverage across the United States, with somewhat inconclusive results. Conversely, it has been demonstrated that trends in total lightning are more robustly correlated to severe weather occurrence, with rapid increases in total lightning observed 10s of minutes prior to the onset of severe weather. Unfortunately, total lightning observations are not as numerous, or available over the same areal coverage domain, as provided by CG networks. Relatively few studies have examined concurrent trends in both total and CG lightning within the same severe thunderstorm, or even large sets of thunderstorms using an objective lightning jump algorithm. Multiple studies have shown that the total flash rate rapidly increases prior to the onset of severe weather. What is untested within the same framework is the use of CG information to perform the same task. Herein, total and CG lightning trends for 711 thunderstorms occurring in four regions of the country were examined to demonstrate the increased utility that total lightning provides over CG lightning, specifically within the framework of developing a useful lightning-based severe weather warning decision support tool. Results indicate that while both lightning datasets demonstrate the presence of increased lightning activity prior to the onset of severe weather, the use of total lightning trends was more effective than CG trends [probability of detection (POD), 79% versus 66%; false alarm rate (FAR), 36% versus 53%; critical success index (CSI), 55% versus 38%; Heidke skill score (HSS), 0.71 versus 0.55]. Moreover, 40% of false alarms associated with total lightning, and 16% of false alarms with CG lightning trends, occurred when a lightning jump associated with a severe weather ''warning'' was already in effect. If these false alarms are removed, the FAR drops from 36% to 22% for total lightning and from 53% to 44% for CG lightning. Importantly, average lead times prior to severe weather occurrence were higher using total lightning as compared with CG lightning (20.65 versus 13.54 min). The ultimate goal of this study was to demonstrate the increased utility of total lightning information that the Geostationary Lightning Mapper (GLM) will provide to operational meteorology in anticipation of severe convective weather on a hemispheric scale once Geostationary Operational Environmental Satellite-R (GOES-R) is deployed in the next decade.

1. Introduction

The electrical energy responsible for lightning flashes in a thunderstorm is intrinsically related to the kinetic energy of the thunderstorm updraft. The updraft provides

Corresponding author address: Christopher J. Schultz, Dept. of Atmospheric Science, National Space Science and Technology Center, University of Alabama in Huntsville, 320 Sparkman Dr., Huntsville, AL 35805.
E-mail: schultz@nsstc.uah.edu

DOI: 10.1175/WAF-D-10-05026.1

© 2011 American Meteorological Society

an environment conducive to mixed-phase microphysical and precipitation processes, associated charge transfer microphysics, cloud-scale separation of charge centers, and attendant large in-cloud electric fields. To discharge excessive buildups of electrical energy resulting in dielectric breakdown, thunderstorms subsequently produce some combination of both intracloud (IC) and cloud-to-ground (CG) lightning flashes. Though total lightning flash rates are most appropriately related to the electrical and hence updraft kinetic energy of a given thunderstorm, it is the CG lightning discharge that poses the largest inherent risk to forests, human safety, and associated infrastructure (e.g., Curran et al. 2000). Hence, numerous CG lightning detection networks have evolved over the past 30 yr [e.g., the U.S. National Lightning Detection Network (NLDN; Cummins et al. 1998; Cummins et al. 2006; Cummins and Murphy 2009), the North American Lightning Detection Network (NALDN; Orville et al. 2002), the Cloud-to-Ground Lightning Surveillance System (CGLASS; Wilson et al. 2009), the Austrian Lightning Detection and Information System (ALDIS; Schulz et al. 2005), and the Brazilian Integrated Lightning Detection Network (RINDAT; Pinto et al. 2006)] to both detect and locate CG lightning flashes in real time. Indeed, when combined with a robust data dissemination infrastructure, these networks do an excellent job of providing nearly instantaneous CG lightning flash location, count, and polarity information to a wide variety of end users.

Given the multidecadal history and relative abundance of CG lightning network data and the reasonable hypothesis that CG lightning flash frequency and thunderstorm intensity should be positively correlated (via the connection of lightning to updraft strength), numerous previous studies have employed network-provided CG lightning information to investigate the application of CG lightning flash data (counts, polarity) to the problem of diagnosing thunderstorm severity. However, the results of these studies have proven to be inconsistent.

Several studies illustrate inconsistency in using CG lightning trends to predict severe weather. Maier and Krider (1982) studied three tornadic storms in Oklahoma and Texas and determined that ''cloud-to-ground lightning location data would have little predictive value for tornadoes,'' when CG rates peaked near the time of tornado dissipation in each case examined. MacGorman et al. (1989) documented a tornadic storm in Oklahoma where the an increase in the IC flash rate occurs prior to tornadogenesis, while the peak CG rate occurs 15 min after the increase in IC lightning and several minutes after the tornado had already touched down. Kane (1991) found two examples where CG lightning rates peaked prior to severe weather in the northeast United States. However, Kane (1991) also cautioned that the examples provided may not be fully representative of the overall storm population and points to Goodman et al. (1988) and Williams et al. (1989) to discuss temporal differences between peak IC rates, CG rates, and maximum outflow. While finding subjective trends in CG lightning prior to tornadogenesis, Knapp (1994) unfortunately did not quantify increases in CG lightning before tornado touchdown in 264 tornadic thunderstorms from across the country. Knapp (1994) did find regional usefulness as to changes in polarity prior to tornado onset. These results were similar to those noted in such studies as Branick and Doswell (1992), Seimon (1993), and MacGorman and Burgess (1994). Curran and Rust (1992) observed a splitting supercell thunderstorm and investigated a polarity reversal from positive to negative flashes in the right-moving component of the split, which ultimately produced a tornado. Bruning et al. (2010) examined a supercell in central Oklahoma and noted a switch in ground flash polarity nearly 10 min in advance of an observed tornado vortex signature on radar; however, no tornado was produced. LaPenta et al. (2005) observed peaks in the CG flash rate nearly 25 min in advance of a tornado in Mechanicville, New York. McCaul et al. (2002) observed a tornadic thunderstorm in Kansas that only produced 17 flashes during its 4.5-h lifetime, while this storm had a peak IC:CG ratio of nearly 700. Perez et al. (1997) found a local peak in CG rates in 74% of F4 and F5 tornado producing thunderstorms between 1989 and 1992. Perez et al. (1997) also stated, ''Similarly, as a singular diagnostic, the occurrence of a peak CG rate offers little predictive value for tornadogenesis in this sample of thunderstorms.'' Carey and Rutledge (1998), Bluestein and MacGorman (1998), Knupp et al. (2003), and Carey et al. (2003) reinforce this idea through the presentation of several tornadic storms that have peak CG rates that vary with respect to tornado occurrence. Furthermore, studies correlating hail and CG trends found that peaks in CG activity occur after hail occurrence (e.g., Changnon 1992; Carey and Rutledge 1996, 1998) or that CG rates in hailstorms are lower than their heavy rain producing counterparts (e.g., Soula et al. 2004). Finally, Maddox et al. (1997) examined microburst-producing thunderstorms in Arizona and observed that many of the most severe convective storms had little if any CG lightning associated with them.

With the more recent advent of VHF total lightning mapping arrays that continuously detect and locate leader sources in the total lightning flash component (IC + CG) over mesoscale regional domains (Williams et al. 1999; Lang et al. 2004; Koshak et al. 2004; MacGorman et al. 2008; Krehbiel 2008), it has now become much easier to evaluate and quantify how well related manifestations of

TABLE 1. Breakdown of thunderstorms in sample by region.

	Tennessee Valley	Mid-Atlantic	OK	STEPS
Severe	205	34	7	9
Nonsevere	350	75	18	13

thunderstorm electrical activity such as the total lightning flash rate (e.g., Gatlin and Goodman 2010; Schultz et al. 2009) perform in a diagnostic sense for severe thunderstorm nowcasting. Moreover, based on the aforementioned physical arguments that relate electrical energy production to thunderstorm draft strength, one would hypothesize that trends in the total lightning flash rate should perform more consistently (as compared to CG lightning) as a tool for severe weather warning decision support. Multiple studies have shown that the total flash rate rapidly increases prior to the onset of severe weather (e.g., Goodman et al. 1988; MacGorman et al. 1989; Williams et al. 1989; Williams et al. 1999; Buechler et al. 2000; Lang et al. 2000; Goodman et al. 2005; Wiens et al. 2005; Steiger et al. 2005; Tessendorf et al. 2007; Steiger et al. 2007; Schultz et al. 2009; Gatlin and Goodman 2010; Darden et al. 2010). What was untested within the same framework was the use of CG information to perform the same task. Indeed, we are not familiar with any particular study in the literature that has taken the step of quantitatively comparing the relationship between severe weather occurrences and associated trends in both the total and CG lightning flash counts for the same large sample of thunderstorms (at least not within the framework of developing a useful lightning-based severe weather warning decision support tool). Accordingly, in this study we present analyses that demonstrate 1) the increased utility of total lightning flash rate tendency as opposed to CG lightning flash tendencies for detecting and nowcasting the occurrence of severe weather and 2) confirm a methodology for applying total lightning flash information to the severe weather nowcasting problem. The results of this study provide further support for the deployment and use of geostationary lightning mappers aboard future geostationary satellite platforms.

2. Methodology

In this section we describe the methodology used to directly compare total (in cloud + cloud to ground; IC + CG) and traditional CG lightning information in order to demonstrate the enhanced information content present in the total lightning data. Our comparisons are set within the framework of an application designed to test the lightning information as an aid for predicting the manifestation of severe weather at the surface. The physical basis for conducting the comparison in this particular manner is that lightning production and severe weather are both closely tied to thunderstorm updrafts, a key characteristic of thunderstorm intensity (e.g., Carey and Rutledge 1996; Carey and Rutledge 1998; Williams et al. 1999; Wiens et al. 2005). Hence, assessment of the relative utility of the respective lightning data types can truly be considered to be a metric for comparison in this specific warning decision support application.

a. Case selection

A collection of 711 thunderstorm cases were analyzed in order to 1) obtain a diverse population of thunderstorm types and 2) attempt to represent what an operational warning forecaster might encounter in various warning decision situations. Both severe thunderstorms (i.e., storms producing tornadoes, hail $\geq$1.9 cm in diameter,[1] or winds $\geq$26 m s^{-1}) and nonsevere thunderstorms are well represented in the database. A total of 1064 severe weather reports were used (133 tornado, 649 hail, and 281 wind), which were combined into 6-min periods and were defined as events for verification purposes discussed below. This method of reducing the number of reports yielded 784 events. The majority of the tornadoes were rated on the lower end of the enhanced Fujita [(E)F] scale, as 76% of tornadoes in this study were (E)F-0 or (E)F-1.

Because the IC:CG flash ratio and convective cell behavior can vary across the country (e.g., Boccippio et al. 2001), different meteorological regimes from four regions of the United States are represented (north Alabama; Washington, D.C.; eastern Colorado–western Kansas; and Oklahoma). North Alabama; Washington, D.C.; and Oklahoma contain operational VHF lightning mapping networks, while total lightning information from eastern Colorado–western Kansas was collected during the Severe Thunderstorm Electrification and Precipitation Study (STEPS; Lang et al. 2004). Each of these regions is also well within the maximum coverage range of the NLDN. A breakdown by region and thunderstorm severity can be found in Table 1. The primary regions of focus, however, are the southeast United States (north Alabama) and mid-Atlantic (Washington, D.C.) due to the ease of access to total lightning data, and to not skew the dataset with regions of the country known to have higher IC:CG ratios (e.g., STEPS; Boccippio et al. 2001;

[1] The minimum size of severe hail recognized by the National Weather Service was increased to 2.54 cm in January 2010; however, for consistency with Schultz et al. (2009) the 1.9-cm definition was retained.

TABLE 2. Breakdown of thunderstorm sample by type. Tropical refers to storms that occur in tropical outer rainbands of landfalling tropical systems, while cold refers to cold season storms.

Type	Supercell	Air mass/multicell	Tropical	Linear	Cold	Low top
Severe	82	73	5	47	38	10
Nonsevere	12	387	4	24	18	11
No.	94	460	9	71	56	21
No. of severe weather events	343	128	8	135	149	18

Lang et al. 2004). Of the 711 thunderstorms, 456 were nonsevere and 255 were severe. An attempt was made to examine as many severe weather producing convective modes as possible from all seasons of the year including supercells, airmass/multicellular convection, linear structures, tornadic outer rainbands of landfalling tropical systems, low-topped convection, and cold season storms.[2] A breakdown of storm types can be found in Table 2.

b. Lightning data

Total lightning datasets in this study were collected using VHF lightning mapping arrays (LMAs; Rison et al. 1999; Krehbiel et al. 2000; Wiens et al. 2005; Goodman et al. 2005; Krehbiel 2008). Four LMA networks were used: north Alabama (NALMA; Koshak et al. 2004; Goodman et al. 2005; Washington, D.C. (DC LMA; Krehbiel 2008); STEPS (Lang et al. 2004); and the Oklahoma Lightning Mapping Array (OK-LMA; MacGorman et al. 2008). For each LMA dataset, VHF source points were combined into flashes using one of two flash-clustering algorithms. For all of the north Alabama thunderstorms, a clustering algorithm developed by McCaul et al. (2005) was implemented. The DC LMA, STEPS, and OK-LMA thunderstorms used a clustering algorithm found in the XLMA software package developed by Thomas et al. (2004) that contains similar spatial criteria. The main difference between the algorithms is that the McCaul et al. (2005) algorithm does not place an upper threshold on the temporal length of a lightning flash; however, both methods produced similar results for the number of lightning flashes detected.

To construct a lightning flash from source data, we required each flash to be composed of a minimum of 10 VHF source points. Thresholding at 10 VHF sources eliminates spurious noise points, which are commonly found in LMA networks. Important to the results of this study, Wiens et al. (2005) demonstrated that applying a source threshold does not affect the general trend in total lightning. All thunderstorms used in this study are within 200 km of the center of each LMA network, due to range limitations of the ground-based LMA networks (e.g., Koshak et al. 2004).

Ground flash counts were determined from the NLDN, which comprises 113 sensors across the United States, and has a flash detection efficiency of 90%–93% (Cummins et al. 2006). The network occasionally misclassifies small in-cloud positive flashes as positive CG flashes; therefore, a +15-kA peak current threshold is applied to accurately estimate cloud-to-ground lightning activity (Biagi et al. 2007; Rudlosky and Fuelburg 2010). No attempt was made to correlate individual CG lightning flashes with the flashes observed using the LMA systems.

c. Lightning jump algorithm selection

Schultz et al. (2009) and Gatlin and Goodman (2010) demonstrated the operational applicability of total lightning jump algorithms in severe weather detection. Schultz et al. (2009) tested six lightning jump algorithm configurations on both nonsevere and severe thunderstorms and determined statistically that the "2σ" configuration held the most promise for an operational algorithm. The algorithm can be summarized in the following steps:

(i) At t_0, the most current 2 min of total lightning data from an individual storm are averaged (see the appendix).[3] This averaging results in units of flashes per minute (flashes min^{-1}).
(ii) If the total flash rate for this thunderstorm is 10 flashes min^{-1}, the algorithm activates. This threshold was determined statistically from a large sample of severe and nonsevere thunderstorms (Schultz et al. 2009).
(iii) Next, the 12 min of total lightning data prior to the most current 2-min time period t_0 is divided into 2-min time periods (i.e., six periods) and averaged as in step i.
(iv) Now, consecutive periods from this 12 min of data are subtracted from each other. This determines the time rate of change of the total flash rate,

[2] Here, we define the cold season storms as having occurred between November and March.

[3] Gatlin and Goodman (2010) determined that 2 min was the most effective period for averaging flash data to eliminate some of the noisiness associated with the total lightning data.

which is referred to as DFRDT. This subtraction results in five DFRDT values.

(v) A standard deviation is then calculated from these five DFRDT values. Twice this value becomes the jump threshold at t_0.

(vi) A new DFRDT value is calculated by subtracting the current total flash rate at t_0, and the flash rate calculated from the 2 min of data just prior to the most recent time, t_{-1}.

(vii) If this DFRDT value exceeds the jump threshold, then a lightning jump has occurred, and a ''warning'' is placed on this thunderstorm for 45 min.

(viii) As additional 2-min time periods of total flash information are received for a particular storm, the process is repeated until the total flash rate drops below the activation threshold of 10 flashes min^{-1}.

The appendix outlines the calculation of this algorithm in additional detail. Performance statistics for the 2σ algorithm exhibited robust values with a probability of detection (POD) of 87%, a false alarm rate (FAR) of 33%, and a Heidke skill score (HSS) of 0.75 (Schultz et al. 2009).

Based on the performance of the 2σ algorithm, the same algorithm configuration of Schultz et al. (2009) was implemented for the total lightning data in this study. For CG lightning information, the algorithm was modified to accommodate lower-frequency cloud-to-ground lightning flash rates. For example, we lowered the threshold to activate the lightning jump algorithm from 10 flashes min^{-1} to 2 flashes min^{-1}, which is consistent with the average CG flash rate of ordinary convection (Williams et al. 1989; Carey and Rutledge 1996; Lang and Rutledge 2002).

Lightning jump times were determined for total and CG lightning using the following procedure. A lightning jump was determined to occur when the value of the flash rate exceeded the trigger threshold and DFRDT exceeded 2σ of the mean DFRDT of the previous 10 min. A jump ends when the DFRDT value is less than or equal to 0, unless two jumps are separated by 6 min or fewer. If two lightning jumps are separated by 6 min or fewer (i.e., jump, no jump, jump), then this is counted as one jump.

d. *Verification and statistical methods*

Similar to the verification methods of Schultz et al. (2009), once a jump in lightning (total or CG) has been detected, a severe warning is placed on the thunderstorm for 45 min. Verification of this warning occurs if severe weather is observed within the warning time period. Severe weather reports that occur within 6 min of each other are counted as one severe weather event. The goal of combining reports is to try and not overstate the algorithm's POD due to well-documented biases in severe weather reporting (e.g., Witt et al. 1998; Williams et al. 1999; Weiss et al. 2002; Trapp et al. 2006). If two warnings are in effect and severe weather is observed, the verification of the severe warning is counted toward the earliest issued warning. Unverified warnings are counted as false alarms, and severe weather events for which no lightning jump is detected are counted as misses. POD, FAR, and critical success index (CSI) are calculated for both lightning data types (Wilks 1995), and an HSS was determined using a formula from Doswell et al. (1990).

3. Results

a. *Case examples*

Boccippio et al. (2001) found that the partitioning of IC and CG activity widely varies across the country. Boccippio et al. (2001) determined IC:CG ratios for the entire CONUS and found the highest IC:CG ratios across the high plains of the United States. Many studies of individual cases from the STEPS field project have supported this finding (e.g., Lang et al. 2004; Wiens et al. 2005; Tessendorf et al. 2007). There are also several studies that have noted high IC:CG ratios or low CG rates in individual severe thunderstorms across the Southeast (e.g., Goodman et al. 1988; Williams et al. 1999; Butts 2006). Three examples are presented below. The first example is what ''typical'' total and CG flash rates would look like in a supercell thunderstorm. However, the purpose of the second and third examples is to show that there are instances where the IC component is considerably larger, while the CG component is virtually nonexistent. The second case presented is from a region where the lack of CG activity can be common and has been documented before (e.g., Tessendorf et al. 2007). However, the purpose of the third example is to demonstrate that larger IC:CG ratios and low CG activity are not confined to the central United States, and can occur in other regions of the country.

1) 7 April 2006, tornadic supercell in northern Alabama

This thunderstorm occurred in northern Alabama during a severe weather outbreak on 7 April 2006, where over 992 severe weather reports were recorded across the Ohio and Tennessee Valleys. Figure 1 depicts an example of a ''typical'' flash rate history of a supercell thunderstorm in the southeast United States during

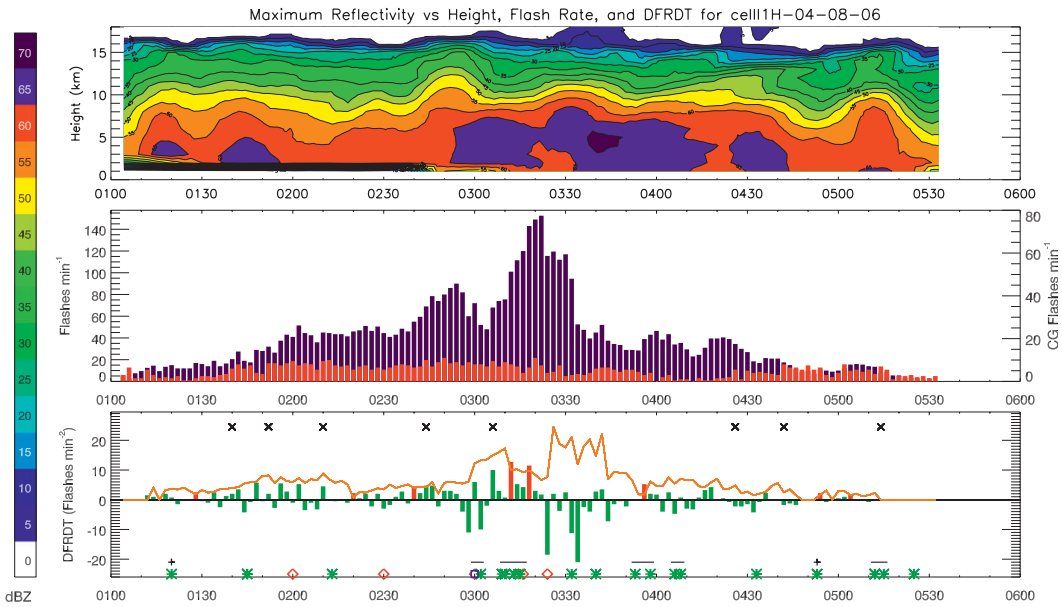

FIG. 1. Time–height plots of (top) maximum reflectivity (dBZ), (middle) lightning rates (flashes min^{-1}), and (bottom) total lightning DFRDT values (flashes min^{-2}) in a supercell thunderstorm in north AL. In the middle plot, total flash counts are represented by purple bars (scale on left), while CG flash counts are represented by red bars (scale on right). In the DFRDT plot, red bars represent total lightning jump times, green bars represent DFRDT values that did not reach the jump threshold, and the 2σ jump threshold is denoted by the orange line. The $\times$ symbols mark where CG lightning jumps occurred, but CG DFRDT trends are not shown. Severe weather reports are located along the bottom of the DFRDT plot (tornado, red diamond; hail, green asterisk; wind, blue square), and symbols with a line over them are grouped into one event. Events with black plus signs above them represent missed events by the total lightning jump algorithm. All but the last total lighting jump were verified by severe weather, while the CG lightning jump had six CG jumps verified and two false alarms (third and eighth). The total lightning jumps preceded 14 of 16 events with this storm, while a CG lightning jump preceded 13 of 16 events.

the storm's lifetime. The peak total flash rate for this thunderstorm was 154 flashes min^{-1}, while the peak CG flash rate was only 14 flashes min^{-1}. Lightning trend information for both total and CG lightning performs very well for this tornadic storm. The total lightning information provides lead times on 14 of 16 severe weather events, while the CG lightning trend information provided lead times on 13 of the 16 severe weather events. The total lightning information provided an average of 23.57 min and the CG lightning trend information provided nearly 19 min of lead time.

2) 20 JUNE 2000, SUPERCELL IN WESTERN KANSAS

This storm (Fig. 2) occurred during the STEPS field project and formed in eastern Colorado around 0030 UTC 20 June 2000. Initially, total flash rates were below 10 flashes min^{-1} with no CG lightning. Between 0045 and 0049 UTC the total flash rate more than tripled from 8 to 26 flashes min^{-1}. Using the 2σ lightning jump algorithm based on the total lightning information, a jump was initiated at 0045 UTC and ended at 0049 UTC. During this same period, no CG lightning was detected and it remained that way until 0059 UTC, when the storm's first CG flash was recorded. At 0104 UTC, approximately 20 min after the triggering of the initial total lightning jump, a wind gust of 75 kt (38.6 m s^{-1}) was recorded by a trained weather spotter.

Four additional total lightning jumps in the total lightning data were indicated by the 2σ algorithm at 0103, 0119, 0141, and 0157 UTC. The largest of these occurred at 0119 UTC, where the total flash rate nearly doubled, increasing from 64 to 108 flashes min^{-1} at 0127 UTC. Additional severe wind damage was reported at 0124, 0142, and 0154 UTC. Interestingly, the CG flash rate for this storm never increased above 2 flashes min^{-1} at any time during the entire storm, there was no evidence of a polarity reversal (only one CG flash was positive), and zero CG lightning jumps were observed during the storm's entire lifetime. Clearly, CG lightning would have been of very limited use in this case. Two false alarms were recorded, and one of these false alarms would have provided additional lead times on two of the wind events; however, lightning jump "warnings" were already in place.

This previous example demonstrates the promise of total lightning information relative to using only CG

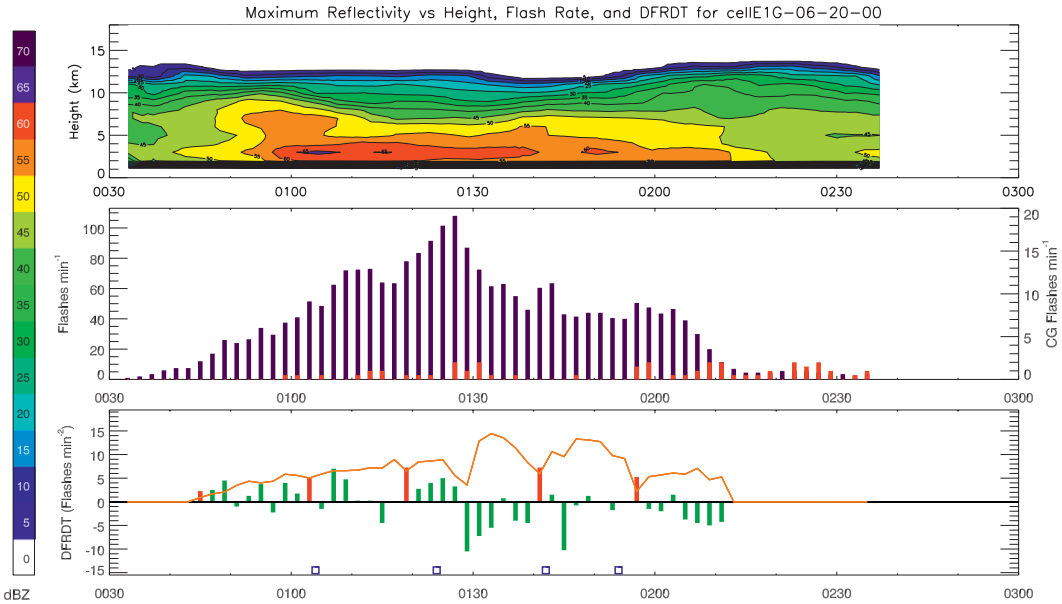

FIG. 2. Same as Fig. 1, but for the severe wind producing thunderstorm from 20 Jun 2000 across western KS. The first three total lightning jumps were verified by severe weather, and the last two were false alarms (one due to a jump already in progress, and the second to a lack of severe weather occurrence after the jump). No CG lightning jumps occurred in this storm.

information. Even though this thunderstorm did not produce many CG flashes (as detected by the NLDN), it was very electrically active—a typical pattern of behavior noted in the events studied. Using the 2σ lightning jump algorithm configuration, total lightning jumps occurred prior to all observed severe weather events for this storm. Furthermore, the average lead time between the total lightning jumps and the severe weather events was 33 min. Because the CG flash rate never exceeded 2 flashes min^{-1} (common to thunderstorms that are nonsevere), all four severe wind events were completely missed when using the CG lightning jump algorithm approach.

3) 18 April 2006, hail-producing supercell thunderstorm in eastern Alabama

On 18 April 2006, a 5-day stretch of severe weather began across the Tennessee Valley. The particular supercell thunderstorm we examine here developed at 2035 UTC 18 April 2006 in Marshall County, Alabama, and for the first hour had the appearance of an ordinary thunderstorm. The total flash rate during this time was below 10 flashes min^{-1} and the peak CG flash rate was 1 flash min^{-1}. At 2140 UTC, the thunderstorm underwent rapid vertical development as indicated by radar (i.e., increases in the height of the 55-dBZ reflectivity contour and the emergence of a 60-dBZ contour; Fig. 3). Between 2146 and 2148 UTC the total flash rate increased from an average of 10 to 18 flashes min^{-1}, and a lightning jump was triggered. The CG flash rate was nonexistent during this time period; indeed, zero CG flashes were detected between 2136 and 2204 UTC. At 2215 UTC the first report of 2.54-cm hail was received at the National Weather Service Forecast Office in Huntsville, Alabama.

At 2218 UTC another total lightning jump occurred as the flash rate increased from 18 to 28 flashes min^{-1}; however, the CG flash rate remained low at only 1 flash min^{-1}. Twenty-six minutes after the 2218 UTC jump (2244 UTC), 3.81-cm hail was observed in Boaz, Alabama. Two additional lightning jumps were observed in the total lightning data (2258 and 2346 UTC), followed by reports of large hail at 2313, 2326, 2342, and 0008 UTC 19 April 2006. Additionally wind damage was reported at 2326 and 0005 UTC. During this 110-min period, the CG flash rate was merely 0.37 flashes min^{-1}.

All six severe weather event periods were accurately identified prior to their occurrence, with an average lead time of 27 min. The CG lightning jump information did not provide any real-time detection of the severe weather events. This is because the CG flash rate was relatively muted, peaking at only 2 flashes min^{-1} with an average flash rate of 0.2 flashes min^{-1} for the entire lifetime of the severe thunderstorm. During the 3 h and 43 min lifetime of this thunderstorm, 56 ground flashes were produced, with only 9 of them of showing positive polarity. The average total lightning flash rate for the lifetime of this storm was a much larger (21 flashes min^{-1}).

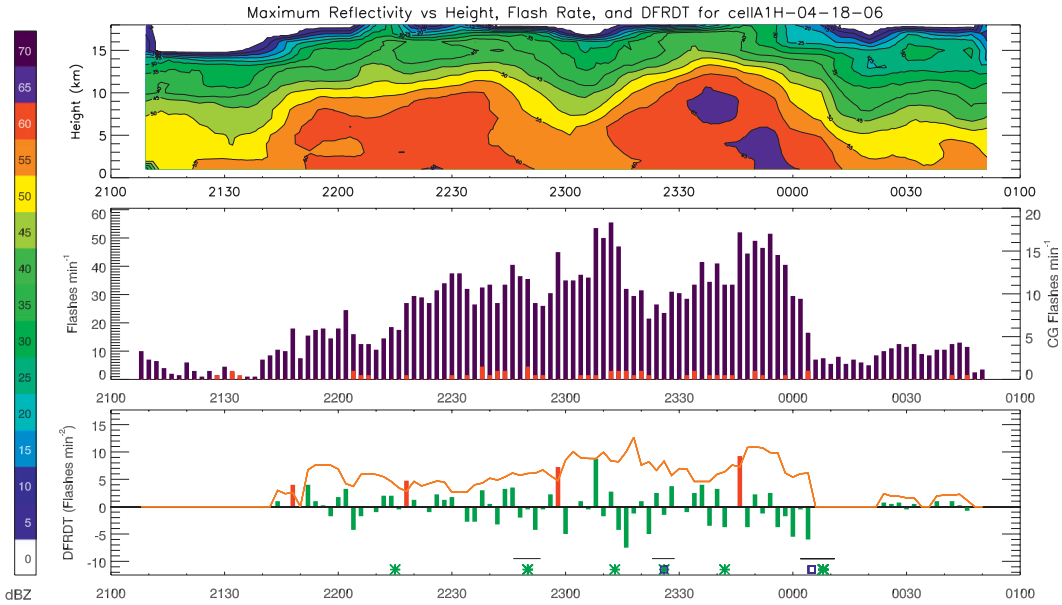

FIG. 3. Same as Fig. 1, but for the hail-producing thunderstorm from 18 Apr 2006 across eastern AL. All four total lightning jumps were verified by severe weather occurrences. No CG lightning jumps occurred in this storm.

b. Summary of performance

Based on the Schultz et al. (2009) study, it is not surprising that the detection of severe weather using the time rate of change of the total flash rate on this sample of 711 thunderstorms worked well. The contingency table statistics yielded a POD of 79%, an FAR of 36%, a CSI of 55%, and an HSS of 0.71 (Table 3). Furthermore, 40% of the false alarms were additional lightning jumps that occurred prior to severe weather observance, but another "warning" was already in place. When these false alarms that still provide lead time on severe weather are removed, the FAR drops to 22%. The average lead time prior to the onset of all severe weather was 20.65 min, with a standard deviation of ±15.05 min. The average lead time on tornadoes alone was 21.32 min with a standard deviation of ±15.15 min.

Conversely, the use of CG lightning trends to diagnose the potential for severe weather on this same set of 711 thunderstorms, while not poor, was not as effective as the use of total lightning trend information. The CG lightning jump algorithm yielded a POD of 66%, an FAR of 53%, a CSI of 38%, and an HSS of 0.55. Sixteen percent of the false alarms occurred when a lightning jump warning was already in place, and if these reports are removed, the FAR drops to 44%. The average lead time for all severe weather using CG lightning was 13.54 min, with a standard deviation of ±15.07 min. The average lead time on tornadoes alone was longer, at 15.24 min with a standard deviation of ±15.27 min.

4. Discussion

The results presented in this study confirm that the use of total lightning information in the 2σ algorithm outperforms a similar algorithm implementation using only CG lightning data. The statistics for the 2σ total lightning jump algorithm were slightly lower than the results of the Schultz et al. (2009) study, but still remained quite strong even given the much larger and more varied sample size of thunderstorm types. Most importantly, this dataset identified specific environments in which the total lightning jump algorithm may need to be altered or combined with previous lightning jump algorithm configurations to enhance utility in low-flashing environments. For example, nearly 40% (64/161) of all missed events by the total lightning 2σ algorithm were from a combination of tropical rainband, cold season, and low-topped storms (Table 4). Similarly, the 2σ algorithm using CG lightning information exhibited similar weaknesses in these environments, as 39% (105/269)

TABLE 3. Skill scores and average lead times using the sample set of 711 thunderstorms for both total lightning and CG lightning, correlating trends in lightning to severe weather.

	POD (%)	FAR (%)	CSI (%)	HSS	Lead time (all, min)	Lead time (tornado, in min)
Total lightning	79	36	55	0.71	20.65	21.32
CG lightning	66	53	38	0.55	13.54	15.24

TABLE 4. Percentage of missed events by thunderstorm type (number of missed events by storm type/total number of events missed) using total and CG lightning information.

Total lightning	Supercell	Air mass/ multicell	Tropical cyclone
	27% (44/161)	17% (28/161)	3% (5/161)
	Linear	Cold season	Low topped
	16% (25/161)	27% (43/161)	16% (16/161)
CG lightning	**Supercell**	**Air mass/ multicell**	**Tropical cyclone**
	46% (125/269)	12% (31/269)	2% (6/269)
	Linear	Cold season	Low topped
	16% (43/269)	19% (50/269)	5% (14/269)

of its misses occurred in these three environments. However, these three storm categories collectively only represented 20% (53/256) of the severe thunderstorm population in this study. Furthermore, nearly 8% of the severe storm population had 0 lightning flashes during their lifetimes, emphasizing that not all severe storms are associated with lightning.

In addition to the three environments discussed above, the CG lightning algorithm missed a significant portion (46%; 125/269) of severe weather events in supercellular thunderstorms (Table 4). In-cloud lightning flash rates peak prior to CG flash rates (e.g., MacGorman et al. 1989; Goodman et al. 2005); thus, a portion of the misses by the CG algorithm occurred during the earlier life cycles of the thunderstorm. Also, there are special cases where no CG flashes are observed, despite large total flash rates (e.g., Tessendorf et al. 2007). The CG lightning jump algorithm performed best with storms that were longer lived, or produced severe weather at the end of their life cycles as the storm dissipated.

These results elucidate a need to continue work on an operational total-lightning jump algorithm; however, it is equally clear that modifications must be made to the current research algorithm to account for low-flashing severe thunderstorm environments in order to enhance the lightning jump algorithm's utility. One of the easiest ways to modify the algorithm would be to lower the flash threshold to activate the algorithm. In cold season and low-topped storms, the average peak total flash rate for severe storms was 11.53 flashes min^{-1}, while that of nonsevere storms in these environments was 6.60 flashes min^{-1}. Thus, lowering the threshold to 6 or 7 flashes min^{-1} may be ideal for cold season and low-topped environments. For landfalling tropical cyclones, any observed total lightning information tended to highlight the most hazardous cells in the outer rainbands. The average peak flash rate in storms that produce tornadoes was 6.60 flashes min^{-1} while the average peak flash rate for those that did not was 0.29 flashes min^{-1}. There were four tornadic rainband storms that produced no lightning; however, if a cell is producing lightning, the likelihood for tornadic potential was increased based on these limited results. Future analysis using a much larger sample of landfalling tropical cyclones will be required to verify this hypothesis.

CG networks will still provide important information on CG ground flash lighting locations and rates and the relatively unambiguous detection of convective storms because the discrimination of CG flashes in GLM optical data is a challenging exercise (Koshak 2010). CG lightning information will still be useful in meteorological applications as it is a key source of information for activities that require this information like human safety, forest fire applications, and infrastructure protection. However, the results presented herein have implications for the use of ground-based CG detection networks relative to either ground (e.g., LMA, LDAR, interferometry, etc.) or space-based total lightning detection equipment. In particular, incorporation of total lightning information should result in improved warnings, lead times, skill scores, more lives saved, and more property protected. Thus, the results of this study firmly support the future utility of total lightning detection instrumentation like the GOES-R Geostationary Lightning Mapper in severe weather warning decision support.

5. Conclusions

The two main goals of this study were to, first, contrast the utility of total and CG lightning occurrence trends in a specific nowcasting application (i.e., a lighting jump algorithm) and, second, to confirm a methodology for applying total lightning flash information to the severe weather nowcasting problem. Examining 711 thunderstorms from four regions of the country and of varying convective modes, we have demonstrated that total lightning trend information outperforms CG lightning trend information. POD (total, 79%; CG, 66%), FAR (total, 36%; CG, 53%), CSI (total, 55%; CG, 38%), HSS (total, 0.71; CG, 0.55) and average lead time of jump occurrence to severe weather occurrence (total, 20.65 min; CG, 13.54 min) were the metrics that separated the two data types in this application of lightning data. Due to the physical relationship between the updraft, precipitation-sized ice; supercooled water; and the initial production of IC flashes within a thunderstorm, total lightning information clearly is the best early indicator of a strengthening updraft within a thunderstorm. CG lightning information, on the other hand, is also still very important for specific meteorological and societal applications (e.g., human safety, forest fire applications, infrastructure protection). Ground-based total lightning networks (e.g.,

LMA, LDAR, interferometry), while highly accurate and useful in a regional setting, are limited in range and costly if expanded out to a global scale. These total lightning networks have very minimal coverage over oceanic regions as well, which are important to aviation and shipping (Cummins and Murphy 2009). Therefore, the results of this study provide further support for the deployment and use of geostationary lightning mappers aboard future GOES satellite platforms.

Acknowledgments. This work was funded by the GOES-R Risk Reduction effort under the Space Act Agreement (NA07AANEG0284). Larry Carey also gratefully acknowledges partial support for this research under an award from the NOAA/NWS CSTAR program (NA08NWS4680034). Walt Petersen and Larry Carey acknowledge partial funding of this research via NOAA's support of the UAH/NSSTC Tornado and Hurricane Observations Research Center (THOR). A special thank you goes out to Dr. Timothy Lang of Colorado State University, Mrs. Stephanie Weiss of the University of Oklahoma, and Dr. Eric Bruning of Texas Tech University for their support of this study by providing lightning mapping array data from the STEPS field project and the OK-LMA network, as well as valuable discussions about the datasets. The authors would also like to acknowledge John Hall and Jeff Bailey for their continued support through maintenance of the NALMA and DCLMA, as well as, Hugh Christian and William Koshak of NASA MSFC for their continued support and advice throughout this study. Finally, the authors would like to acknowledge three anonymous reviewers for helping to improve the quality of this manuscript.

APPENDIX

Calculation of DFRDT and the 2σ Algorithm

The 2σ algorithm is a multiple-step process that uses the most recent flash history of a thunderstorm to identify when thunderstorm intensification is ongoing. The first step is combining two 1-min flash periods and averaging them over a 2-min period using

$$\mathrm{FR}_{\mathrm{avg}}(t_i)(\text{flashes min}^{-1}) = \frac{\mathrm{FR}_{t1}(t_1) + \mathrm{FR}_{t2}(t_2)}{2}. \quad \text{(A1)}$$

This helps to eliminate some of the noisiness found within the lightning data and has been shown to be the most effective time averaging technique by Gatlin and Goodman (2010). The second step in the algorithm requires a total flash rate of 10 flashes min^{-1} before starting any jump calculations. This was based on a sample set of thunderstorms and is outlined in Schultz et al. (2009), and also eliminates smaller jumps associated with typical nonsevere convection, which cause false alarms. Next, a time rate of change of the flash rate (DFRDT) is calculated using

$$\frac{d}{dt}\mathrm{FR}_{\mathrm{avg}}(t_{i+1}) = \frac{\mathrm{FR}_{\mathrm{avg}}(t_{i+1}) - \mathrm{FR}_{\mathrm{avg}}(t_i)}{t_{i+1} - t_i} = \mathrm{DFRDT}(\text{flashes min}^{-2}). \quad \text{(A2)}$$

Fourth, a standard deviation value is calculated based on the most previous five periods of DFRDT values prior to the current 2-min time period. The jump threshold for the 2σ algorithm is twice this standard deviation. Thus, if the most recent DFRDT value exceeds twice this standard deviation, a jump has been identified, and a ''warning'' is placed on the storm of interest for the next 45 min for verification purposes.

REFERENCES

Biagi, C. J., K. L. Cummins, K. E. Kehoe, and E. P. Krider, 2007: National Lightning Detection Network (NLDN) performance in southern Arizona, Texas and Oklahoma in 2003–2004. *J. Geophys. Res.,* **112,** D05208, doi:10.1029/2006JD007341.

Bluestein, H. B., and D. R. MacGorman, 1998: Evolution of cloud-to-ground lightning characteristics and storm structure in the Spearman, Texas, tornadic supercells of 31 May 1990. *Mon. Wea. Rev.,* **126,** 1451–1467.

Boccippio, D. J., K. L. Cummins, H. J. Christian, and S. J. Goodman, 2001: Combined satellite- and surface-based estimation of the intracloud-to-ground lightning ratio over the continental United States. *Mon. Wea. Rev.,* **129,** 108–129.

Branick, M. L., and C. A. Doswell III, 1992: An observation of the relationship between supercell structure and lightning ground-strike polarity. *Wea. Forecasting,* **7,** 143–149.

Bruning, E. C., W. D. Rust, D. R. MacGorman, M. I. Biggerstaff, and T. J. Schurr, 2010: Formation of charge structures in a supercell. *Mon. Wea. Rev.,* **138,** 3740–3761.

Buechler, D. E., K. T. Driscoll, S. J. Goodman, and H. J. Christian, 2000: Lightning activity within a tornadic thunderstorm observed by the Optical Transient Detector (OTD). *Geophys. Res. Lett.,* **27,** 2253–2256.

Butts, D. A., Jr., 2006: An examination of the relationship between cool season tornadoes and cloud-to-ground lightning flashes. M.S. thesis, Dept. of Atmospheric Sciences, Texas A&M University, 109 pp.

Carey, L. D., and S. A. Rutledge, 1996: A multiparameter radar case study of the microphysical and kinematic evolution of a lightning producing storm. *Meteor. Atmos. Phys.,* **59,** 33–64.

——, and ——, 1998: Electrical and multiparameter radar observations of a severe hailstorm. *J. Geophys. Res.,* **103,** 13 979–14 000.

——, W. A. Petersen, and S. A. Rutledge, 2003: Evolution of cloud-to-ground lightning and storm structure in the Spencer, South Dakota, tornadic supercell of 30 May 1998. *Mon. Wea. Rev.,* **131,** 1811–1831.

Changnon, S. A., 1992: Temporal and spatial relations between hail and lightning. *J. Appl. Meteor.,* **31,** 587–604.

Cummins, K. L., and M. J. Murphy, 2009: An overview of lightning location systems: History, techniques, and data uses with an

in-depth look at the U.S. NLDN. *IEEE Trans. Electromagn. Compat.,* **51,** 499–518.

——, ——, E. A. Bardo, W. L. Hiscox, R. B. Pyle, and A. E. Pifer, 1998: A combined TOA/MDF technology upgrade of the U.S. National Lightning Detection Network. *J. Geophys. Res.,* **103,** 9035–9044.

——, J. A. Cramer, C. J. Biagi, E. P. Krider, J. Jerauld, M. A. Uman, and V. A. Rakov, 2006: The U.S. National Lightning Detection Network: Post-upgrade status. Preprints, *Second Conf. on Meteorological Applications of Lightning Data,* Atlanta, GA, Amer. Meteor. Soc., 6.1. [Available online at http://ams.confex.com/ams/pdfpapers/105142.pdf.]

Curran, E. B., and W. D. Rust, 1992: Positive ground flashes produced by low-precipitation thunderstorms in Oklahoma on 26 April 1984. *Mon. Wea. Rev.,* **120,** 544–553.

——, R. L. Holle, and R. E. Lopez, 2000: Lightning casualties and damages in the United States from 1959 to 1994. *J. Climate,* **13,** 3448–3464.

Darden, C. B., D. J. Nadler, B. C. Carcione, R. J. Blakeslee, G. T. Stano, and D. E. Buechler, 2010: Utilizing total lightning information to diagnose convective trends. *Bull. Amer. Meteor. Soc.,* **91,** 167–175.

Doswell, C. A., III, R. Davies-Jones, and D. L. Keller, 1990: On summary of skill in rare event forecasting based on contingency tables. *Wea. Forecasting,* **5,** 576–585.

Gatlin, P. N., and S. J. Goodman, 2010: A total lightning trending algorithm to identify severe thunderstorms. *J. Atmos. Oceanic Technol.,* **27,** 3–22.

Goodman, S. J., D. E. Buechler, P. D. Wright, and W. D. Rust, 1988: Lightning and precipitation history of a microburst-producing storm. *Geophys. Res. Lett.,* **15,** 1185–1188.

——, and Coauthors, 2005: The North Alabama Lightning Mapping Array: Recent severe storm observations and future prospects. *Atmos. Res.,* **76,** 423–437.

Kane, R. J., 1991: Correlating lightning to severe local storms in the northeastern United States. *Wea. Forecasting,* **6,** 3–12.

Knapp, D., 1994: Using cloud-to-ground lightning data to identify tornadic thunderstorm signatures and nowcast severe weather. *Natl. Wea. Dig.,* **19** (2), 35–42.

Knupp, K. R., S. Paech, and S. Goodman, 2003: Variations in cloud-to-ground lightning characteristics among three adjacent tornadic supercell storms over the Tennessee Valley region. *Mon. Wea. Rev.,* **131,** 172–188.

Koshak, W. J., 2010: Optical characteristics of OTD flashes and the implications for flash-type discrimination. *J. Atmos. Oceanic Technol.,* **27,** 1822–1838.

——, and Coauthors, 2004: North Alabama Lightning Mapping Array (LMA): VHF source retrieval algorithm and error analysis. *J. Atmos. Oceanic Technol.,* **21,** 543–558.

Krehbiel, P. R., 2008: The DC Lightning Mapping Array. Preprints, *Third Conf. on Meteorological Applications of Lightning Data,* New Orleans, LA, Amer. Meteor. Soc., 3.2. [Available online at http://ams.confex.com/ams/pdfpapers/129095.pdf.]

——, R. J. Thomas, W. Rison, T. Hamlin, J. Harlin, and M. Davis, 2000: GPS-based mapping system retrieval of lightning inside storms. *Eos, Trans. Amer. Geophys. Union,* **81,** 21–25.

Lang, T. J., and S. A. Rutledge, 2002: Relationships between convective storm kinematics, precipitation, and lightning. *Mon. Wea. Rev.,* **130,** 2492–2506.

——, ——, J. E. Dye, M. Venticinque, P. Laroche, and E. Defer, 2000: Anomalously low negative cloud-to-ground lightning flash rates in intense convective storms observed during STERAO-A. *Mon. Wea. Rev.,* **128,** 160–173.

——, and Coauthors, 2004: The Severe Thunderstorm Electrification and Precipitation Study (STEPS). *Bull. Amer. Meteor. Soc.,* **85,** 1107–1125.

LaPenta, K. D., L. F. Bosart, T. J. Galarneau, and M. J. Dickinson, 2005: A multiscale examination of the 31 May 1998 Mechanicsville, New York, tornado. *Wea. Forecasting,* **20,** 494–516.

MacGorman, D. R., and D. W. Burgess, 1994: Positive cloud-to-ground lightning in tornadic storm and hailstorms. *Mon. Wea. Rev.,* **122,** 1671–1697.

——, ——, V. Mazur, W. D. Rust, W. L. Taylor, and B. C. Johnson, 1989: Lightning rates relative to tornadic storm evolution on 22 May 1981. *J. Atmos. Sci.,* **46,** 221–250.

——, and Coauthors, 2008: TELEX: The Thunderstorm Electrification and Lightning Experiment. *Bull. Amer. Meteor. Soc.,* **89,** 997–1013.

Maddox, R. A., K. W. Howard, and C. L. Dempsey, 1997: Intense convective storms with little or no lightning over central Arizona: A case of inadvertent weather modification? *J. Appl. Meteor.,* **36,** 302–314.

Maier, M. W., and E. P. Krider, 1982: A comparative study of cloud-to-ground lightning characteristics in Florida and Oklahoma thunderstorms. Preprints, *12th Conf. on Severe Local Storms,* San Antonio, TX, Amer. Meteor. Soc., 334–337.

McCaul, E. W., Jr., D. E. Buechler, S. Hodanish, and S. J. Goodman, 2002: The Almena, Kansas, tornadic storm of 3 June 1999: A long-lived supercell with very little cloud-to-ground lightning. *Mon. Wea. Rev.,* **130,** 407–415.

——, J. Bailey, S. J. Goodman, R. Blakeslee, and D. E. Buechler, 2005: A flash clustering algorithm for North Alabama Lightning Mapping Array data. Preprints, *Conf. on Meteorological Applications of Lightning Data,* San Diego, CA, Amer. Meteor. Soc., 5.3. [Available online at http://ams.confex.com/ams/pdfpapers/84373.pdf.]

Orville, R. E., G. R. Huffines, W. R. Burrows, R. L. Holle, and K. L. Cummins, 2002: The North American Lightning Detection Network (NALDN)—First results: 1998–2000. *Mon. Wea. Rev.,* **130,** 2098–2109.

Perez, A. H., L. J. Wicker, and R. E. Orville, 1997: Characteristics of cloud-to-ground lightning associated with violent tornadoes. *Wea. Forecasting,* **12,** 428–437.

Pinto, O., Jr., K. P. Naccarato, I. R. C. A. Pinto, W. A. Fernandes, and O. P. Neto, 2006: Monthly distribution of cloud-to-ground lightning flashes as observed by lightning location systems. *Geophys. Res. Lett.,* **33,** L09811, doi:10.1029/2006GL026081.

Rison, W., R. J. Thomas, P. R. Krehbiel, T. Hamlin, and J. Harlin, 1999: A GPS-based three dimensional lightning mapping system: Initial observations in central New Mexico. *Geophys. Res. Lett.,* **26,** 3573–3576.

Rudlosky, S. D., and H. E. Fuelburg, 2010: Pre- and postupgrade distributions of NLDN reported cloud-to-ground lightning characteristics in the contiguous United States. *Mon. Wea. Rev.,* **138,** 3623–3633.

Schultz, C. J., W. A. Petersen, and L. D. Carey, 2009: Preliminary development and evaluation of lightning jump algorithms for the real-time detection of severe weather. *J. Appl. Meteor. Climatol.,* **48,** 2543–2563.

Schulz, W., K. Cummins, G. Diendorfer, and M. Dorninger, 2005: Cloud-to-ground lightning in Austria: A 10-year study using data from a lightning location system. *J. Geophys. Res.,* **110,** D09101, doi:10.1029/2004JD005332.

Seimon, A., 1993: Anomalous cloud-to-ground lightning in an F5-tornado-producing supercell thunderstorm on 28 August 1990. *Bull. Amer. Meteor. Soc.,* **74,** 189–203.

Soula, S., Y. Seity, L. Feral, and H. Sauvageot, 2004: Cloud-to-ground lightning activity in hail-bearing storms. *J. Geophys. Res.,* **109,** D02101, doi:10.1029/2003JD003669.

Steiger, S. M., R. E. Orville, M. J. Murphy, and N. W. S. Demetriades, 2005: Total lightning and radar characteristics of supercells: Insights on electrification and severe weather forecasting. Preprints, *Conf. on the Meteorological Application of Lightning Data,* San Diego, CA, Amer. Meteor. Soc., P1.7. [Available online at http://ams.confex.com/ams/pdfpapers/84908.pdf.]

——, ——, and L. D. Carey, 2007: Total lightning signatures of thunderstorm intensity over north Texas. Part I: Supercells. *Mon. Wea. Rev.,* **135,** 3281–3302.

Tessendorf, S. A., K. C. Wiens, and S. A. Rutledge, 2007: Radar and lightning observations of the 3 June 2000 electrically inverted storm from STEPS. *Mon. Wea. Rev.,* **135,** 3665–3681.

Thomas, R. P., P. R. Krehbiel, W. Rison, S. Hunyady, W. Winn, T. Hamlin, and J. Harlin, 2004: Accuracy of the lightning mapping array. *J. Geophys. Res.,* **109,** D14207, doi:10.1029/2004JD004549.

Trapp, R. J., D. M. Wheatly, N. T. Atkins, and R. W. Przybylinkski, 2006: Buyer beware: Some words of caution on the use of severe wind reports in postevent assessment and research. *Wea. Forecasting,* **21,** 408–415.

Weiss, S. J., J. A. Hart, and P. R. Janish, 2002: An examination of severe thunderstorm wind report climatology: 1970–1999. Preprints, *21st Conf. on Severe Local Storms,* San Antonio, TX, Amer. Meteor. Soc., 446–449.

Wiens, K. C., S. A. Rutledge, and S. A. Tessendorf, 2005: The 29 June 2000 supercell observed during STEPS. Part II: Lightning and charge structure. *J. Atmos. Sci.,* **62,** 4151–4177.

Wilks, D. S., 1995: *Statistical Methods in the Atmospheric Sciences*. Academic Press, 467 pp.

Williams, E. R., M. E. Weber, and R. E. Orville, 1989: The relationship between lightning type and convective state of thunderclouds. *J. Geophys. Res.,* **94,** 13 213–13 220.

——, and Coauthors, 1999: The behavior of total lightning activity in severe Florida thunderstorms. *Atmos. Res.,* **51,** 245–265.

Wilson, J. G., K. L. Cummins, and E. P. Krider, 2009: Small negative cloud-to-ground lightning reports at the NASA Kennedy Space Center and Air Force Eastern Range. *J. Geophys. Res.,* **114,** D24103, doi:10.1029/2009JD012429.

Witt, A., M. D. Eilts, G. J. Stumpf, E. D. Mitchell, J. T. Johnson, and K. W. Thomas, 1998: Evaluating the performance of WSR-88D severe storm detection algorithms. *Wea. Forecasting,* **13,** 513–518.